CORROSION PERFORMANCE OF STRUCTURAL ALLOYS FOR OXY-FUEL COMBUSTION SYSTEMS

K. Natesan and D. L. Rink
Argonne National Laboratory, 9700 South Cass Avenue, Argonne, IL 60439
E-mail: natesan@anl.gov; Telephone: (630) 252-5103; Fax: (630) 252-8681

ABSTRACT

The U.S. Department of Energy (DOE) Office of Fossil Energy is intensely promoting research and development of oxyfuel combustion systems that employ oxygen, instead of air, for burning the fuel. The resulting flue gas primarily consists of H_2O and CO_2 that facilitates sequestration of CO_2, thereby leading to reduction in CO_2 emissions. Also, as the oxidant is bereft of N_2, NO_x emissions are minimized to a great extent from the exhaust gas. Studies at NETL have indicated that oxy-fuel combustion can increase efficiency in the power plants from the current 30-35% to 50-60%. However, the presence of H_2O/CO_2 and trace constituents like nitrogen and sulfur in the environment at the operating temperatures and pressures can have adverse effects on the corrosion and mechanical properties of structural alloys. Thus, there is a critical need to evaluate the response of structural and turbine materials in simulated H_2O/CO_2 environments in an effort to select materials that have adequate high temperature mechanical properties and environmental performance.

During the past year, a program was initiated to evaluate the corrosion performance of structural alloys in CO_2 and CO_2-steam environments at elevated temperatures. Materials selected for the study include intermediate-chromium ferritic steels, Fe-Cr-Ni heat-resistant alloys, and nickel-based superalloys. Coupon specimens of several of the alloys were exposed to pure CO_2 at temperatures between 650 and 850°C for times up to 1450 h. The corrosion tests in CO_2-50% steam environment was conducted at temperatures between 650 and 850°C for times up to 1250 h. The steam for the experiment was generated by pumping distilled water and converting it to steam in the preheat portion of the furnace, ahead of the specimen exposure location. Preliminary results will be presented on weight change, scale thickness, internal penetration, and microstructural characteristics of corrosion products.

BACKGROUND

An increase in carbon dioxide gas in the atmosphere is identified as one of the major causes for the global climate change and one of the source of carbon dioxide is the exhaust from fossil fuel fired combustion power plants. The energy production, in particular electricity generation, is expected to increase due to population increase and per capita increase in energy consumption. To meet the energy needs, fossil fuels (coal, oil, and gas) will play a major part in production even with a projected increase in alternate renewable sources. However, to minimize the carbon dioxide emission, the current systems emphasize capture from power plants and subsequent sequestartion. The oxy-fuel combustion systems can enable recycling of the carbon dioxide to the compressor, use of novel gas turbines, and advance reuse.

The U.S. department of Energy Office of Fossil Energy is supporting the development of combustion systems replacing air with nearly pure oxygen with a goal to achieving a near zero-emission coal-based power system. For this purpose turbines and combustor technologies that use pure oxygen in fuel combustion are being developed. The major advantage of combustion under pure oxygen is the potential for separation and capture of CO_2 and for achieving power system efficiencies in the range of 50 to 60%.

Clean Energy Systems, Inc. (CES) has developed zero-emission fossil-fueled power generation technology, integrating proven aerospace technology into conventional power systems. The core of CES' process involves replacing conventional steam boilers and exhaust gas cleaning systems with "gas generator" technology adapted from rocket engines. The gas generator burns a combination of gaseous oxygen and any gaseous fuel composed primarily of the elements carbon, hydrogen, and oxygen (C-H-O), including natural gas, landfill gas, or syngas from coal, refinery residues or biomass. The combustion is performed at essentially stoichiometric conditions in the presence of recycled water to produce a mixed gas of steam and carbon dioxide (CO_2) at high temperature and pressure.

The first generation zero-emission power projects are also considering use of the effluent from oxy-fuel combustion in a gas turbine to generate electricity. For example, in the ongoing Zero Emission Norwegian Gas (ZENG) Project in Norway plans to identify the requirements to modify a gas turbine to work on the steam/Co2 mixture. Specifically, the study examines capability of turbines that could support a 200 MWe plant using the oxy-fuel combustion system.

The objective of this work is to evaluate the oxidation and corrosion performance of structural and gas turbine alloys in CO_2 and steam/CO_2 environments over a wide temperature range. Further, the goal is to establish the kinetics of scaling and internal penetration, if any, and develop correlations for long term performance of the alloys. Eventually, the influence of the exposure environment on the mechanical properties, especially creep, fatigue, and creep fatigue, of the candidate alloys needs evaluation.

EXPERIMENTAL PROCEDURE

MATERIALS

The compositions of the Fe-base alloys selected for the study are listed in Table 1. Numerous alloys, both ASME coded and uncoded, were selected for corrosion evaluation. The alloys included advanced ferritic steel modified 9Cr-1Mo, The included austenitic Fe-alloys were Type 304 and 330 stainless steel and Alloy 800H. In addition, several high-Ni alloys (333, 617, 625, 602CA, 230, 693, 740, and 718) were included in the study, especially for application at temperatures above 700°C. MA956 is a Fe-Cr alloy produced by powder metallurgy route via high-energy ball milling and subsequent extrusion.

OXIDATION/CORROSION EXPERIMENTS

Two different experimental systems were used for the oxidation in CO_2 and in steam-CO_2 environments. The experiments in CO2 were conducted in a three-zone, resistance-heated furnace that contained 35-mm O.D. quartz reaction tube, which was closed at the bottom (se

Table 1. Nominal composition (in wt.%) of alloys selected for corrosion study

Material	C	Cr	Ni	Mn	Si	Mo	Fe	Other
Modified 9Cr	0.10	9	0.8	0.5	0.4	1.0	Bal	Nb 0.08, V 0.20, N 0.06
304	0.08	18.0	8.0	1.6	0.6	-	Bal	
800H	0.08	20.1	31.7	1.0	0.2	0.3	Bal	Al 0.4, Ti 0.3
330	0.05	10.0	35.0	1.5	1.25	-	Bal	
333	0.05	25.0	45.0	-	1.0	3.0	18.0	Co 3.0, W 3.0
617	0.08	21.6	53.6	0.1	0.1	9.5	0.9	Co 12.5, Al 1.2, Ti 0.3
625	0.05	21.5	Bal	0.3	0.3	9.0	2.5	Nb 3.7, Al 0.2, Ti 0.2
602CA	0.19	25.1	62.6	0.1	0.1	-	9.3	Al 2.3, Ti 0.13, Zr 0.19, Y 0.09
230	0.11	21.7	60.4	0.5	0.4	1.4	1.2	W 14, Al 0.3, La 0.015
693	0.02	28.8	Bal	0.2	0.04	0.13	5.8	Al 3.3, Nb 0.67, Ti 0.4, Zr 0.03
740	0.07	25.0	Bal	0.3	0.5	0.5	1.0	Co 20.0, Ti 2.0, Al 0.8,, Nb+Ta 2.0
718	-	19.0	52.0	-	-	3.0	19.0	Nb 5.0, Al 0.5, Ti 0.9, B 0.002
MA956	-	20.0	-	-	-	-	Bal	Al 4.5, Ti 0.5, Y_2O_3 0.6

Figure 1. Photograph of experimental set up for oxidation tests in a CO_2 environment

Fig.1). The alloy samples were polished with 600-grit SiC abrasive paper and rinsed with ethyl alcohol. The specimens were attached to a 5-mm O.D. thermocouple well located in the center of each reaction tube. Carbon dioxide gas entered through a 5-mm O.D. quartz tube attached to the inside of the reaction tube, passed through the sample section, and exited at the top. The temperature in the vicinity of the samples was controlled to within ~1°C. The dimensions and weight of the test coupons were determined before and after exposure to the gas environment.

A tubular resistance-heated furnace (see Fig. 2) was used to expose coupon specimens of the alloys to flowing mixture of steam and CO_2. The system consists of a furnace with a constant temperature zone of ≈20 cm and a reaction chamber made of high-purity alumina. The steam for the experiment was generated by pumping distilled water and converting it to steam in the preheat portion of the furnace, ahead of the specimen exposure location. The exhaust steam from the chamber was condensed in a steam condenser. The flow rate was 6 cc/h of water. A mass balance on the water flow showed that almost all the input water was collected as the effluent, indicating that the steam consumption was negligible during the oxidation of specimens. Argon gas was used to disperse the steam in the reaction chamber.

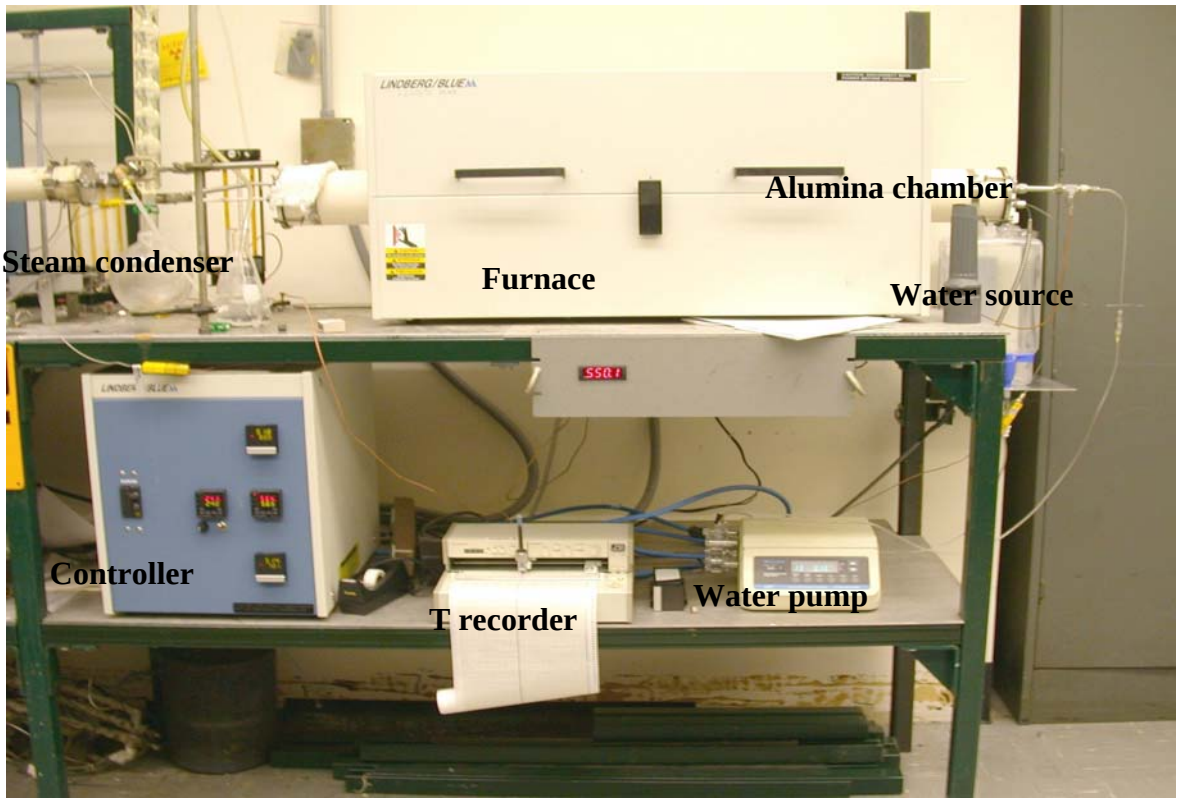

Figure 2. Test facility used for oxidation of alloys in steam/CO_2 environments.

Upon completion of the exposures, the specimen surfaces were analyzed using a scanning electron microscope equipped with an energy dispersive X-ray analyzer. In addition to weight change in specimens, microscopy of the cross sections of the exposed specimens was used to establish the internal penetration, if any, into the substrate of the various specimens.

RESULTS AND DISCUSSION

OXIDATION PERFORMANCE

Specimens were exposed to pure carbon dioxide gas for 1452 h at temperatures of 650, 750, and 850°C. The specimens were retrieved periodically to measure the weight change and re-exposed

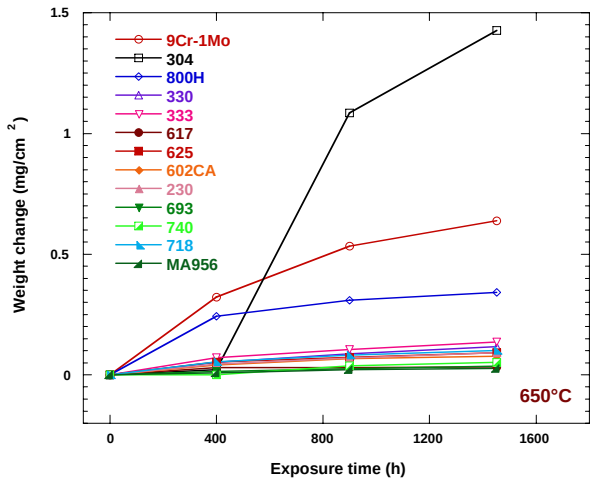

Figure 3. Weight change for alloys after exposure in CO_2 at 650°C.

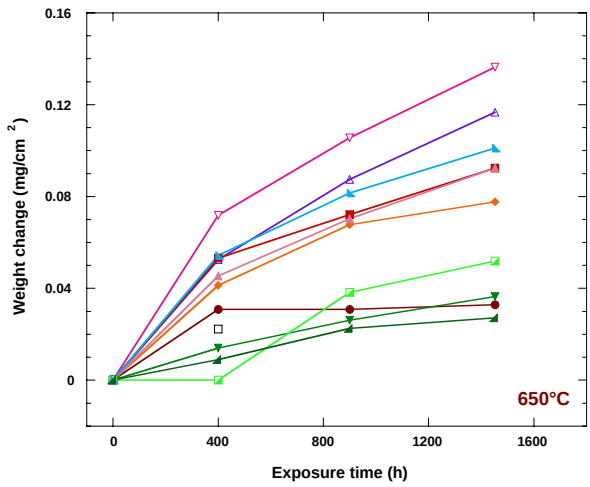

Figure 4. Magnified view of the data in Fig. 3.

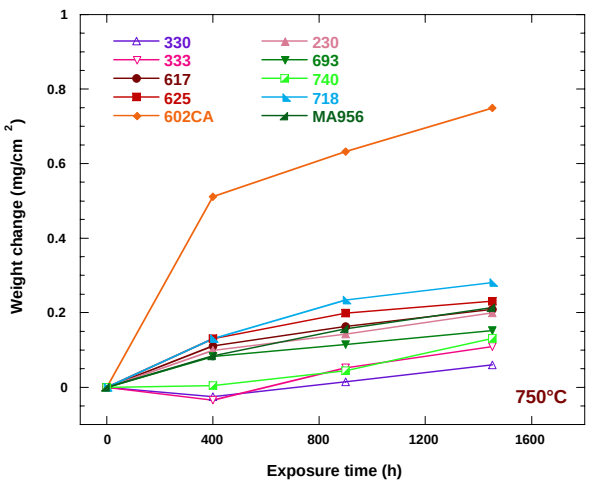

Figure 5. Weight change for alloys after exposure in CO_2 at 750°C.

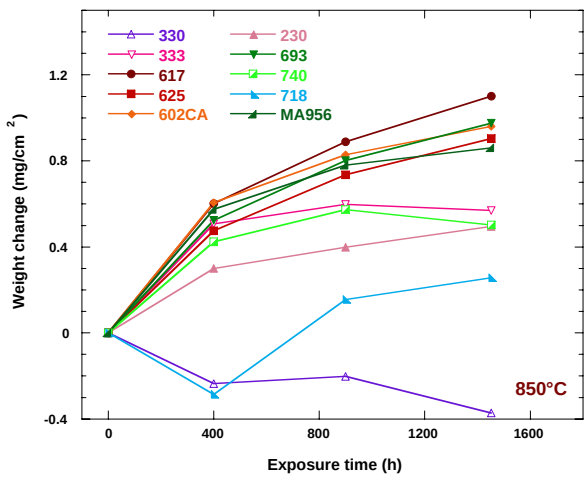

Figure 6. Weight change for alloys after exposure in CO_2 at 850°C.

for longer time. Figure 3 shows the weight change data for several alloys after exposure at 650°C. Figure 4 shows a magnified view of the data in Fig. 3 to differentiate the oxidation performance of alloys that are bunched together in Fig. 3. Figures 5 and 6 show the weight change data for alloys that were tested at 750 and 850°C. The data indicate a increase in weight change by factors of 2-3 and 7-10 at exposure temperatures of 750 and 850°C when compared with those observed at 650°C.

Specimens were also exposed to 50% steam-50% carbon dioxide environment for 1865 h at 650°C and for 2760 h at 750°C. The test at 850°C is currently in progress. The specimens in these tests were also retrieved periodically to measure the weight change and re-exposed for longer time. Figure 7 shows the weight change data for several alloys after exposure at 650°C. Figure 8 shows a magnified view of the data in Fig. 7. Figure 9 shows the weight change data

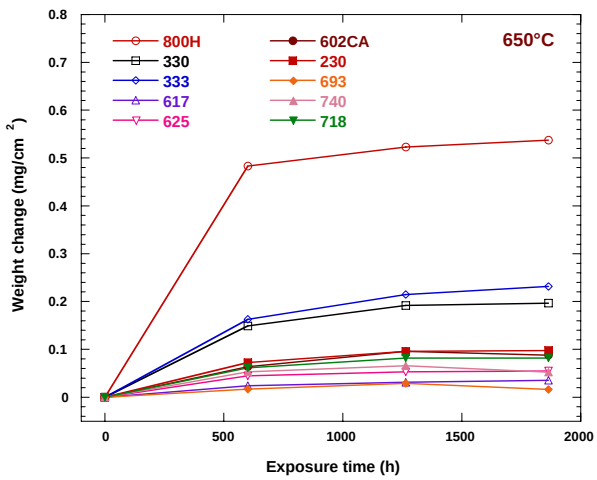

Figure 7. Weight change for alloys after exposure in 50% steam-50% CO_2 at 650°C.

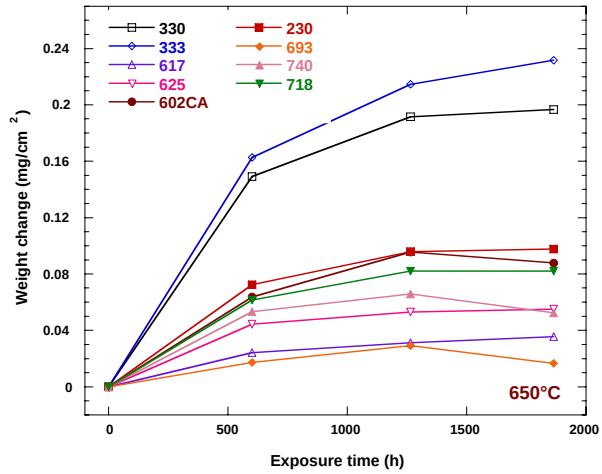

Figure 8. Magnified view of the data in Fig. 7.

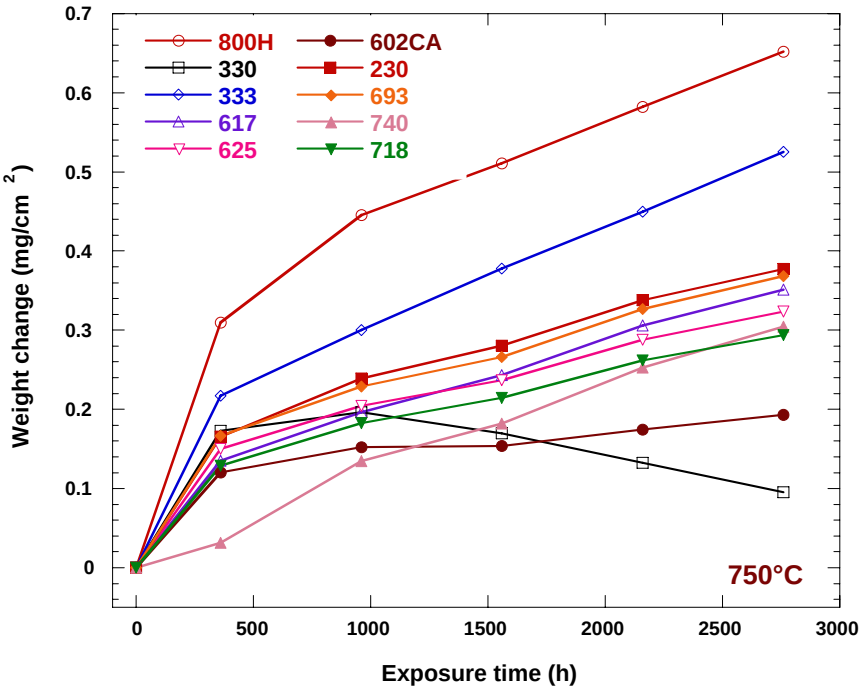

Figure 9. Weight change for alloys after exposure in 50% steam-50% CO_2 at 750°C.

for the alloys tested at 750°C in steam-CO_2 environment. The data indicate that the weight change is about a factor of three greater at 750°C when compared with those at 650°C.

Figure 10 shows a comparison of weight change data obtained in pure CO2 and in 50% steam-50% CO2 environments at 750°C. Preliminary indications are that the initial oxidation rate in steam-CO2 mixture is somewhat faster than in pure CO_2. Additional tests are in progress and the entire database will be used to compare the oxidation performance of the alloys as a function of temperature, steam content, and alloy chemistry.

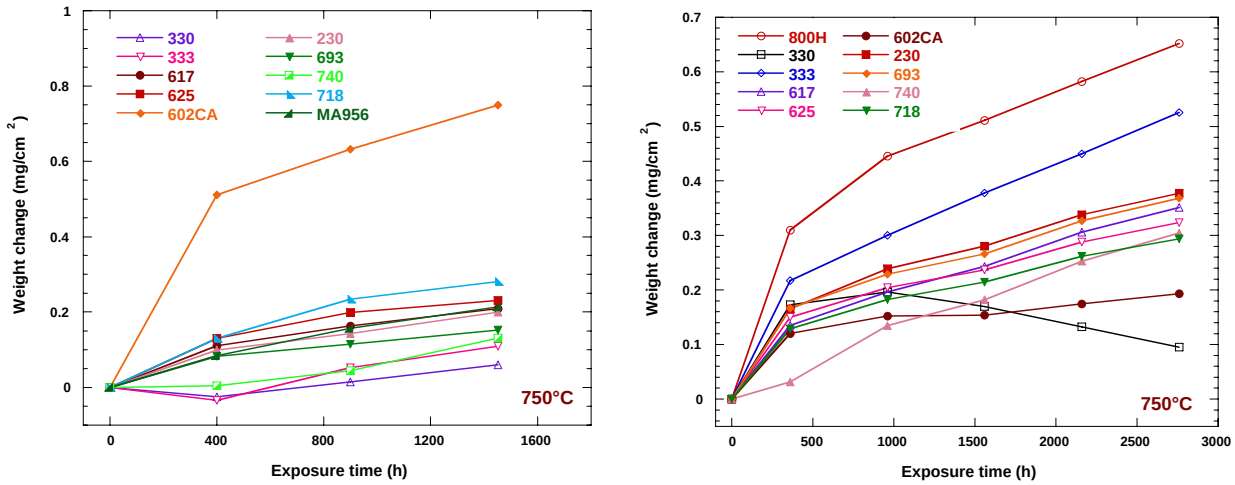

Figure 10. Weight change for alloys after exposure in (left) pure CO_2 and (right) 50% steam-50% CO_2 environments at 750°C.

MICROSTRUCTURAL OBSERVATIONS

Extensive analysis is in progress to evaluate the microstructural characteristics of the scales and internal penetration, if any, of the alloys after exposure in CO_2 and in steam-CO_2 environments.

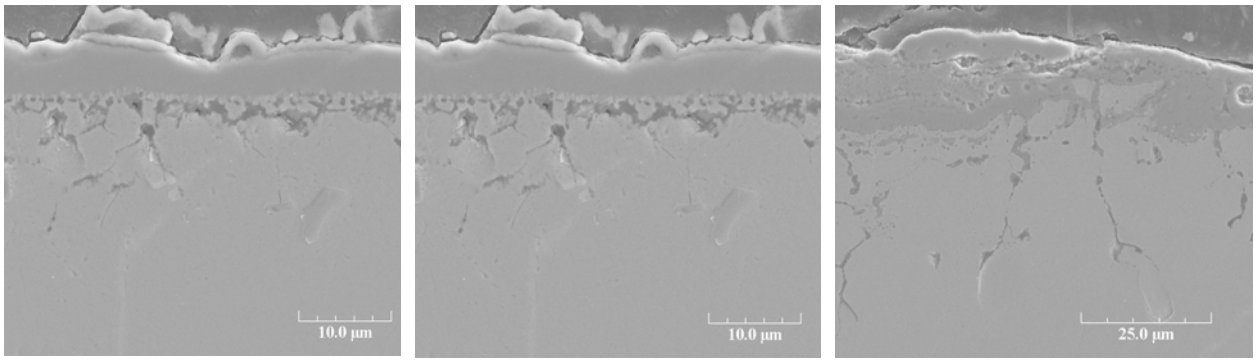

(a) (b) (c)

Figure 11. SEM photomicrographs of Ally 800H (un-etched) after exposure 1452-h exposure in CO2 gas at (a) 650, (b) 750, and (c) 850°C.

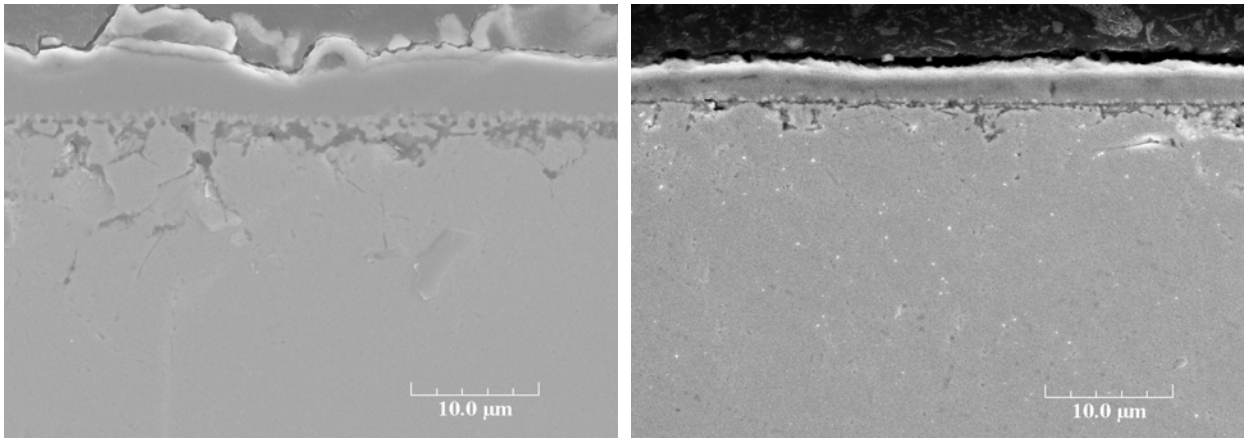

(a) (b)

Figure 12. Scanning electron photomicrographs of cross sections of Alloy 800H (un-etched) after exposure at 750°C in (a) pure CO_2 for 1452 h and (b) 50% steam-50% CO_2 for 960 h.

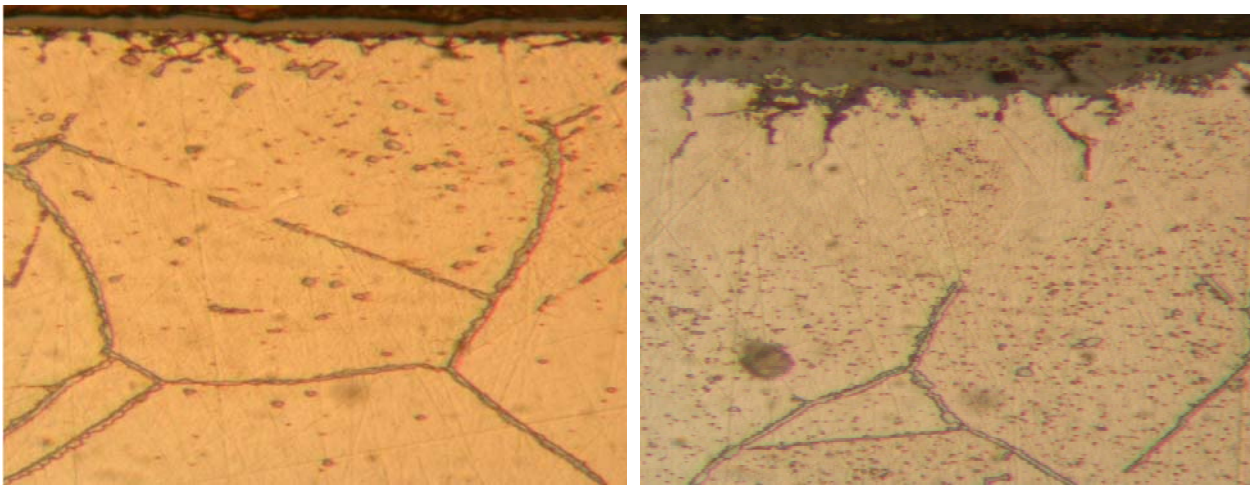

(a) (b)

Figure 13. SEM photomicrographs of Ally 800H (un-etched) after exposure 1452-h exposure in CO_2 gas at (a) 750, and (b) 850°C.

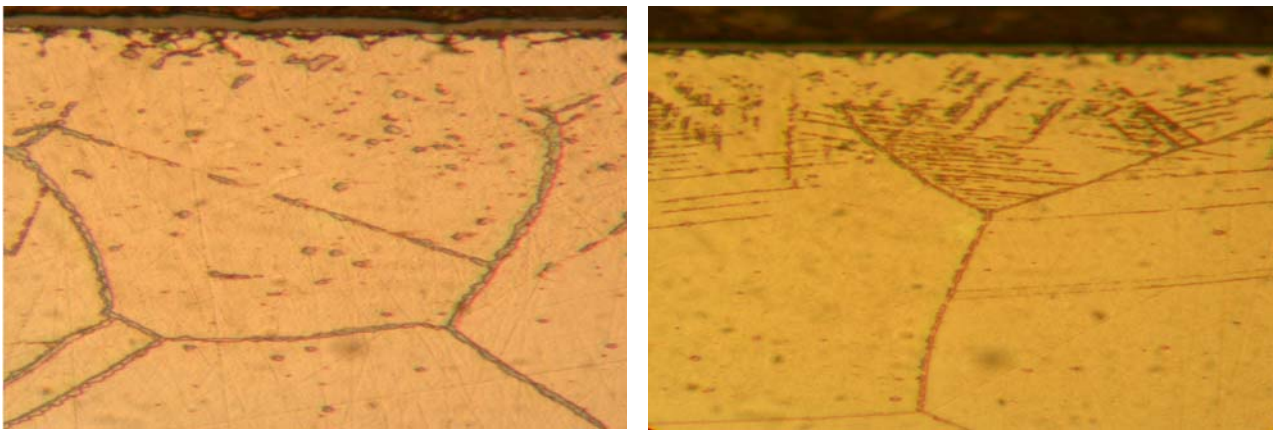

(a) (b)

Figure 14. SEM photomicrographs of Ally 800H (etched) after exposure at 750°C in (a) CO_2 gas for 1452 h and (b) 50% steam-50% CO_2 mixture for 960 h.

We next address the thermodynamic aspects of metal corrosion in a bioxidant situation, such as an oxygen/carbon environment. The following surface reactions are possible on a divalent metal A:

$$A + 1/2\ O_2 = AO, \tag{21}$$

$$A + C = AC, \tag{22}$$

where AO and AC are the oxide and carbide reaction products, respectively. Under equilibrium conditions, the partial pressures of oxygen and activity of carbon are defined by the relations

$$(a_O)_{eq} = pO_2^{1/2} = \exp(\Delta G_{AO}/RT), \tag{23}$$

$$(a_C)_{eq} = \exp(\Delta G_{AC}/RT), \tag{24}$$

where ΔG_{AO} and ΔG_{AC} are the standard free energies of formation of the oxide and carbide, respectively, at temperature T. From Eqs. (23) and (24), one should be able to deduce the conditions for oxidation or carburization; however, a further reaction must be considered, namely

$$AC + 1/2\ O_2 = AO + C, \tag{25}$$

with the equilibrium condition

$$(a_C/a_O)_{eq} = \exp[(\Delta G_{AC} - \Delta G_{AO})/RT]\ a_{AC}/a_{AO}. \tag{26}$$

If we assume unit activity for the phases AC and AO, Eq. (26) is reduced to

$$(a_C/a_O)_{eq} = \exp[(\Delta G_{AC} - \Delta G_{AO})/RT]. \tag{27}$$

Examination of Eqs. (23), (24), and (27) permits the identification of various situations that limit the type of surface corrosion products that can be formed, as follows:

(i) $$\text{if } (a_O)_{gas} > (a_O)_{eq} \text{ and } (a_C)_{gas} < (a_C)_{eq}, \tag{28}$$

then AO is the only stable surface phase;

(ii) $$\text{if } (a_O)_{gas} < (a_O)_{eq} \text{ and } (a_C)_{gas} > (a_C)_{eq}, \tag{29}$$

then AC is the only stable surface phase; and

(iii) $$\text{if } (a_O)_{gas} > (a_O)_{eq} \text{ and } (a_C)_{gas} > (a_C)_{eq}, \tag{30}$$

then both AO and AC should be stable and form as surface products. However, reference to Eq. (25) indicates that only one phase will form, depending on which of the following conditions prevails:

(a) $$(a_C/a_O)_{gas} > (a_C/a_O)_{eq}, \quad (31)$$

(b) $$(a_C/a_O)_{gas} < (a_C/a_O)_{eq}. \quad (32)$$

Condition (a) will cause Eq. (25) to proceed to the left, and AC will be the stable phase where the metal is in contact with the gas phase. In condition (b), AO will be the stable phase, and Eq. (25) will proceed to the right.

A convenient way of representing the possible corrosion products as a function of gas chemistry is to construct thermochemical diagrams that depict the stability ranges of various condensed phases as functions of the thermodynamic activities of the two components of the reactive gas. Figure 3.3 shows a thermochemical stability diagram for the Cr–C–O system developed for a temperature of 982°C. In the construction of this diagram, the thermodynamic activities of the metal and corrosion–product phases are assigned a value of unity. In multicomponent alloys, the activities of constituent elements will be less than unity and should be accounted for in the analysis. Further, in gas/solid reactions that involve multicomponent alloys, a more complex corrosion product (i.e., more complex than a binary compound) can result that would decrease the thermodynamic activities of the specific phase in the mixture.

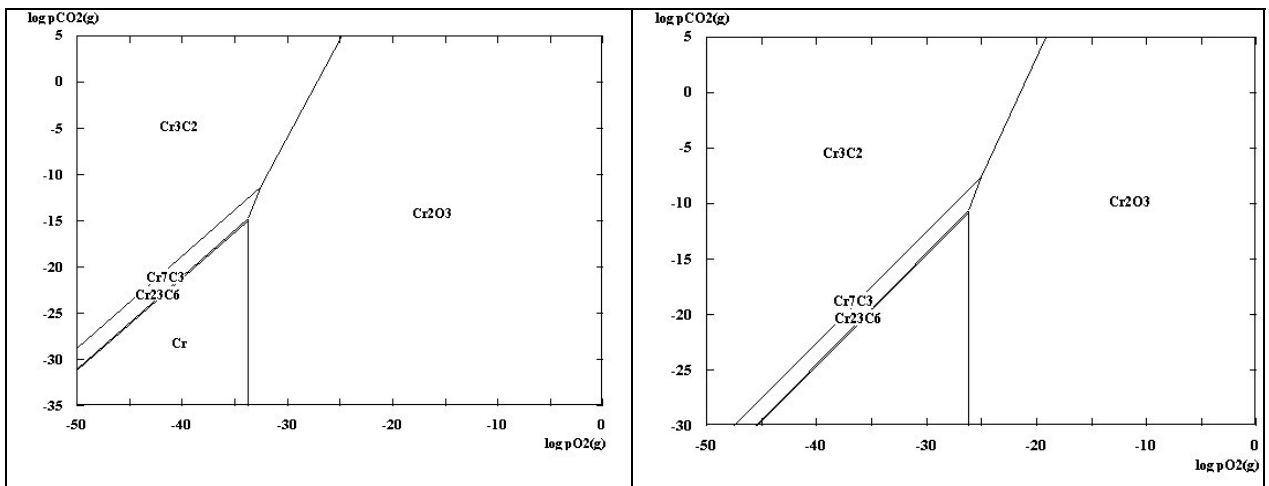

(a) (b)

Figure 12. Scanning electron photomicrographs of cross sections of Alloy 800H (un-etched) after exposure at 750°C in (a) pure CO_2 for 1452 h and (b) 50% steam-50% CO_2 for 960 h.

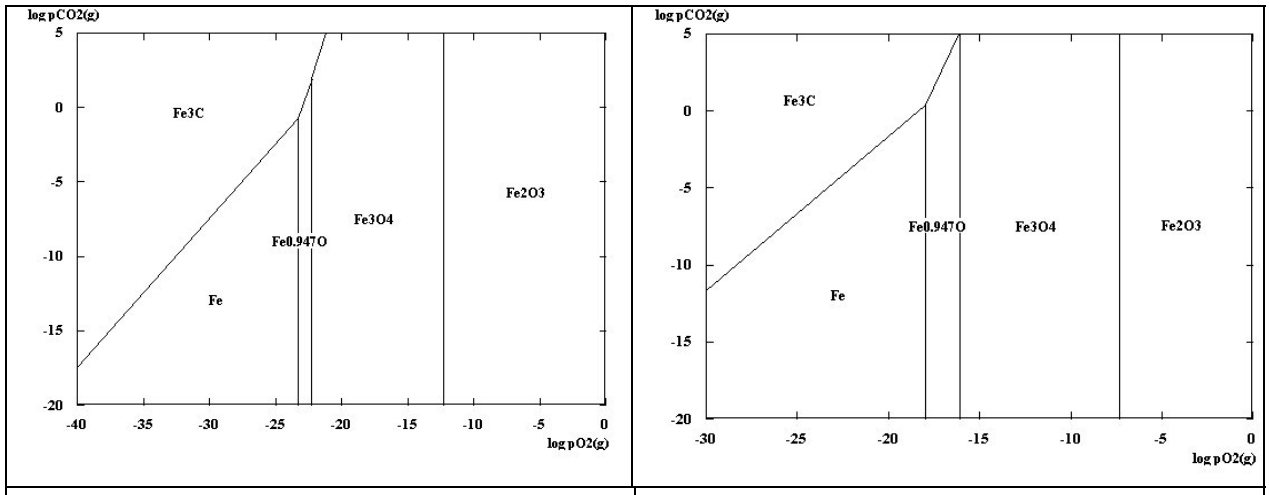

(a) (b)

Figure 12. Scanning electron photomicrographs of cross sections of Alloy 800H (un-etched) after exposure at 750°C in (a) pure CO_2 for 1452 h and (b) 50% steam-50% CO_2 for 960 h.

We have initiated a study to evaluate the oxidation performance of structural alloys in CO_2 and CO_2-steam environments at temperatures up to 1000°C

We will incorporate additional gas-turbine alloys as they become available

The preliminary results indicate that the oxide scales that develop on the alloys are not that protective and internal carburization of the substrate can occur

The internal carbon diffusion accompanied by carbide precipitation can be modeled to predict the long term performance of the alloys

The carburization, even though looks subtle, can have significant degrading effect on the mechanical properties such as, creep rupture, fatigue, and creep fatigue

ACKNOWLEDGEMENTS

This work was supported by the U.S. Department of Energy, Office of Fossil Energy, Advanced Research Materials Program, Work Breakdown Structure Element ANL–4, under Contract DE-AC02-06CH11357.

REFERENCES

R. E. Anderson, S. E. Doyle, and K. L. Pronske, "Demonstration and Commercialization of Zero-Emission Power Plants," 29th International Technical Conference on Coal Utilization & Fuel Systems, April 18-22, 2004, Clearwater, FL.